Measurements of the Proton and Deuteron Spin Structure Function g_2 and Asymmetry A_2

K. Abe,[15] T. Akagi,[12,15] P. L. Anthony,[12] R. Antonov,[11] R. G. Arnold,[1] T. Averett,[16,*] H. R. Band,[17] J. M. Bauer,[7] H. Borel,[5] P. E. Bosted,[1] V. Breton,[3] J. Button-Shafer,[7] J. P. Chen,[16] T. E. Chupp,[8] J. Clendenin,[12] C. Comptour,[3] K. P. Coulter,[8] G. Court,[12,†] D. Crabb,[16] M. Daoudi,[12] D. Day,[16] F. S. Dietrich,[6] J. Dunne,[1] H. Dutz,[12,‡] R. Erbacher,[12,13] J. Fellbaum,[1] A. Feltham,[2] H. Fonvieille,[3] E. Frlez,[16] D. Garvey,[9] R. Gearhart,[12] J. Gomez,[4] P. Grenier,[5] K. A. Griffioen,[11,§] S. Hoibraten,[16,||] E. W. Hughes,[12,*] C. Hyde-Wright,[10] J. R. Johnson,[17] D. Kawall,[13] A. Klein,[10] S. E. Kuhn,[10] M. Kuriki,[15] R. Lindgren,[16] T. J. Liu,[16] R. M. Lombard-Nelsen,[5] J. Marroncle,[5] T. Maruyama,[12] X. K. Maruyama,[9] J. McCarthy,[16] W. Meyer,[12,‡] ,[1] Z.-E. Meziani,[13,14] R. Minehart,[16] J. Mitchell,[4] J. Morgenstern,[5] G. G. Petratos,[12,¶] R. Pitthan,[12] D. Pocanic,[16] C. Prescott,[12] R. Prepost,[17] P. Raines,[11] B. Raue,[10] D. Reyna,[1] A. Rijllart,[12,**] Y. Roblin,[3] L. S. Rochester,[12] S. E. Rock,[1] O. A. Rondon,[16] I. Sick,[2] L. C. Smith,[16] T. B. Smith,[8] M. Spengos,[1] F. Staley,[5] P. Steiner,[2] S. St.Lorant,[12] L. M. Stuart,[12] F. Suekane,[15] Z. M. Szalata,[1] H. Tang,[12] Y. Terrien,[5] T. Usher,[12] D. Walz,[12] J. L. White,[1] K. Witte,[12] C. C. Young,[12] B. Youngman,[12] H. Yuta,[15] G. Zapalac,[17] B. Zihlmann,[2] and D. Zimmermann[16]

(E143 Collaboration)

[1]*The American University, Washington, D.C. 20016*
[2]*Institut für Physik der Universität Basel, CH-4056 Basel, Switzerland*
[3]*LPC IN2P3/CNRS, University Blaise Pascal, F-63170 Aubiere Cedex, France*
[4]*CEBAF, Newport News, Virginia 23606*
[5]*DAPNIA-Service de Physique Nucleaire Centre d'Etudes de Saclay, F-91191 Gif-sur-Yvette, France*
[6]*Lawrence Livermore National Laboratory, Livermore, California 94550*
[7]*University of Massachusetts, Amherst, Massachusetts 01003*
[8]*University of Michigan, Ann Arbor, Michigan 48109*
[9]*Naval Postgraduate School, Monterey, California 93943*
[10]*Old Dominion University, Norfolk, Virginia 23529*
[11]*University of Pennsylvania, Philadelphia, Pennsylvania 19104*
[12]*Stanford Linear Accelerator Center, Stanford, California 94309*
[13]*Stanford University, Stanford, California 94305*
[14]*Temple University, Philadelphia, Pennsylvania 19122*
[15]*Tohoku University, Sendai 980, Japan*
[16]*University of Virginia, Charlottesville, Virginia 22901*
[17]*University of Wisconsin, Madison, Wisconsin 53706*
(Received 26 September 1995)

We have measured proton and deuteron virtual photon-nucleon asymmetries A_2^p and A_2^d and structure functions g_2^p and g_2^d over the range $0.03 < x < 0.8$ and $1.3 < Q^2 < 10$ (GeV$/c)^2$ by inelastically scattering polarized electrons off polarized ammonia targets. Results for A_2 are significantly smaller than the positivity limit $\sqrt{R}$ for both targets. Within experimental precision the g_2 data are well described by the twist-2 contribution, $g_2^{\rm WW}$. Twist-3 matrix elements have been extracted and are compared to theoretical predictions.

PACS numbers: 13.60.Hb, 13.88.+e, 24.70.+s, 25.30.Fj

The nucleon spin structure functions $g_1(x, Q^2)$ and $g_2(x, Q^2)$ are important tools for testing QCD, models of nucleon structure, and sum rules. Experiments at CERN [1,2] and SLAC [3–5] have measured g_1 and g_2 using deep inelastic scattering (DIS) of longitudinally polarized leptons on polarized nuclear targets. These studies have largely concentrated on g_1^p, g_1^d, and g_1^n, which are dominant when the target is polarized along the beam direction. Their results have established that the quark component of the nucleon helicity is much smaller than the naive quark-parton model predictions [6]. In addition, the Bjorken sum rule [7], a fundamental QCD prediction for the difference of the first moments of g_1^p and g_1^n, has been confirmed within the uncertainties of experiments and theory [2,3,5]. This sum rule has also been used to extract the QCD coupling constant α_s at low Q^2 [8].

The present work concentrates on $g_2^p(x, Q^2)$ and $g_2^d(x, Q^2)$ which are dominant when longitudinally polarized leptons scatter from transversely polarized nucleons. The g_2 structure function probes both transverse and longitudinal parton polarization distributions inside the nucleon. Properties of g_2 have been established using the operator product expansion (OPE) within QCD [9,10], and the interpretation of g_2 in the light-cone parton model is on firm grounds [11–13]. There are twist-2 (evolves logarithmically in Q^2) and twist-3 (suppressed by an additional $1/\sqrt{Q^2}$) contributions to g_2 which can be written

$$g_2(x,Q^2) = g_2^{\mathrm{WW}}(x,Q^2) - \int_x^1 \frac{\partial}{\partial y}\left(\frac{m}{M}h_T(y,Q^2) + \xi(y,Q^2)\right)\frac{dy}{y}\,. \tag{1}$$

The twist-2 part comes from $g_2^{\mathrm{WW}}(x,Q^2)$ and the quark transverse polarization distribution $h_T(x,Q^2)$, while the twist-3 part $\xi(x,Q^2)$ comes from quark-gluon interactions. The Bjorken scaling variable is denoted by x, $-Q^2$ is the four-momentum transfer squared, m and M are quark and nucleon masses, and y is the x-integration variable. The g_2^{WW} expression of Wandzura-Wilczek [14],

$$g_2^{\mathrm{WW}}(x,Q^2) = -g_1(x,Q^2) + \int_x^1 \frac{g_1(y,Q^2)}{y}\,dy\,, \tag{2}$$

can be derived from the OPE [9,10] sum rules for g_1 and g_2 at fixed Q^2,

$$\int_0^1 x^n g_1(x,Q^2)dx = \frac{a_n}{2}, \quad n = 0,2,4,\ldots,$$

$$\int_0^1 x^n g_2(x,Q^2)dx = \frac{1}{2}\,\frac{n}{n+1}(d_n - a_n), \quad n = 2,4,\ldots \tag{3}$$

by keeping a_n (twist-2) and neglecting the d_n (twist-3) matrix elements of the renormalized operators. The quantity $h_T(x,Q^2)$ in Eq. (1) contributes to leading order in quark-quark scattering (e.g., polarized Drell-Yan processes), but is suppressed by m/M [12,13,15] in DIS. This component should not be confused with the twist-3 quark mass term that appears in the OPE nor with the average transverse spin [15,16] $g_T = g_1 + g_2$ that measures the spin distribution normal to the virtual photon momentum.

The OPE analysis does not yield a sum rule for the first moment of g_2 ($n = 0$). However, Burkhardt and Cottingham [17] have derived the sum rule $\int_0^1 g_2(x)dx = 0$ in the $Q^2 \to \infty$ limit from virtual Compton scattering dispersion relations. Due to the uncertainty in the very small x behavior of g_2, it may not be possible to experimentally test this sum rule [9,18].

The spin asymmetries A_1 and A_2 for virtual Compton scattering are directly related to the spin structure functions. From the virtual photon transverse cross section σ_T and the transverse-longitudinal interference cross section σ^{TL}, one can form the transverse asymmetry

$$A_2(x,Q^2) = \frac{\sigma^{TL}}{\sigma^T} = \frac{(Q/\nu)[g_1(x,Q^2) + g_2(x,Q^2)]}{F_1(x,Q^2)}\,, \tag{4}$$

where E and E' are the incident and scattered lepton energies, $\nu = E - E'$, and $F_1(x,Q^2)$ is a spin-averaged DIS structure function. The SMC has measured A_2^p [2] (see Fig. 1) at four values of x in the range $0.006 \le x \le 0.6$ and $1 < Q^2 < 30$ (GeV$/c)^2$. These results are much closer to zero than the positivity condition $|A_2(x,Q^2)| \le \sqrt{R(x,Q^2)}$, where $R(x,Q^2)$ is the ratio of longitudinal to transverse virtual photon absorption cross sections.

In this paper, we report on measurements of the proton and deuteron asymmetries A_2^p and A_2^d and the transverse structure functions g_2^p and g_2^d from SLAC experiment E143 over the range $1.3 < Q^2 < 10$ (GeV$/c)^2$ and $0.029 < x < 0.8$. Results for g_1^p and g_1^d from this experiment as well as details on the experiment and data analysis have been previously reported [4,5]. Longitudinally polarized electrons with energy 29.1 GeV were scattered from polarized protons and deuterons in cryogenic ammonia targets into two independent spectrometers at angles of 4.5° and 7°. The targets could be polarized longitudinally or transversely relative to the beam by physically rotating the polarizing magnet. The measured asymmetries were calculated from the difference over the sum of rates for scattering longitudinally polarized electrons with negative and positive beam helicities from transversely ($A_\perp$) and longitudinally ($A_\parallel$) polarized targets. The most significant corrections to the asymmetries were made for the beam polarization which was measured with a Møller polarimeter to be typically 0.85 ± 0.02; the target polarizations which were typically 0.65 ± 0.017 for protons and 0.25 ± 0.011 for deuterons; the fraction of polarizable protons or deuterons

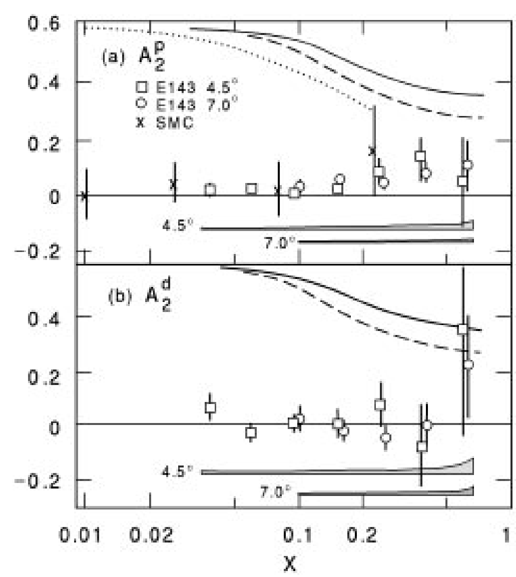

FIG. 1. Measurements for (a) A_2^p and (b) A_2^d from E143 (two data sets) and SMC as a function of x. Systematic errors are indicated by bands. The curves show the $\sqrt{R}$ [22] positivity constraints. The solid, dashed, and dotted curves correspond to the 4.5° E143, 7.0° E143, and SMC kinematics, respectively. Overlapping data have been shifted slightly in x to make errors clearly visible.

which ranged from 0.12 to 0.17 for $^{15}NH_3$ and from 0.22 to 0.24 for $^{15}ND_3$; the contribution from polarized nitrogen nuclei and for residual polarized protons in the ND_3 target; and the radiative corrections which include internal [19] and external [20] contributions. These x-dependent radiative corrections typically shifted A_2 by $+0.01$. The corresponding shift in g_2 was $+0.30$ at low x, decreasing rapidly to $+0.002$ at high x. The systematic errors for the radiative corrections to $A_\perp$ were typically as large as the corrections themselves and were dominated by the uncertainty in the model for $g_2(x, Q^2)$.

Both A_2 and g_2 can be expressed in terms of the experimental asymmetries as

$$A_2(x, Q^2) = \frac{\gamma(2 - y)}{2d}\left[A_\perp \frac{y(1 + xM/E)}{(1 - y)\sin\theta} + A_\parallel\right],$$

$$g_2(x, Q^2) = \frac{yF_1(x, Q^2)}{2d}\left[\frac{E + E'\cos\theta}{E'\sin\theta} A_\perp - A_\parallel\right], \tag{5}$$

where $\gamma = 2Mx/\sqrt{Q^2}$, θ is the scattering angle, $y = (E - E')/E$, $d = (1 - \epsilon)(2 - y)/y[1 + \epsilon R(x, Q^2)]$, and $\epsilon^{-1} = 1 + 2[1 + \gamma^{-2}]\tan^2(\theta/2)$. For $F_1(x, Q^2) = F_2(x, Q^2)(1 + \gamma^2)/2x[1 + R(x, Q^2)]$, we used fits to data for F_2 [21] and for R [22] which was extrapolated to unmeasured regions for $x < 0.08$. All results were calculated using 28 x bins for 4.5° and 20 x bins for 7°. For the figures, every four bins were combined by error weighted averaging.

Results for A_2^p and A_2^d are shown in Fig. 1. The error bars are statistical only. Systematic errors, dominated by radiative correction uncertainties, are indicated by bands. For a given x, the Q^2 probed by the two spectrometers differs by nearly a factor of two. Also in Fig. 1 are proton results from SMC [2] and the $\sqrt{R}$ [22] positivity limits for each data set. The data are much closer to zero than the positivity limit, although A_2^p is consistently >0. The average value for A_2^p for both data sets (ignoring possible Q^2 dependence) is 0.030 ± 0.009. Note that A_2 is expected to be zero at $Q^2 \to \infty$ because $R \to 0$. It has been suggested [23] that the Q^2 dependence of A_2 is of the form $1/\sqrt{Q^2}$ which is not measurable within the precision of the data shown here.

Measurements of xg_2 for the proton and deuteron are shown in Fig. 2. The g_2^d results are per nucleon. The systematic errors are indicated by bands. Also shown is the g_2^{WW} curve evaluated using Eq. (2) at $E = 29$ GeV and $\theta = 4.5°$. We determined g_2^{WW} using $g_1(x, Q^2)$, evaluated from a fit to world data of A_1 [24] and assuming negligible higher-twist contributions. Also shown are bag model predictions [16,25] which include twist-2 and twist-3 contributions for $Q^2 = 5$ (GeV$/c)^2$. At high x the results for g_2^p indicate a negative trend consistent with the expectations for g_2^{WW}. Comparing the proton data to the hypothesis $g_2 = 0$ yields a χ^2 of 52 for 48 degrees of freedom (DOF), while comparing to the hypothesis $g_2 = g_2^{WW}$ yields a χ^2 of 43. The corresponding confidence levels for agreement with the hypotheses are 32% and 67%, respectively. The deuteron results are less conclusive because of the larger errors. The χ^2 tests for $g_2 = 0$ and $g_2 = g_2^{WW}$ yield similar χ^2 values of about 45 for 48 DOF.

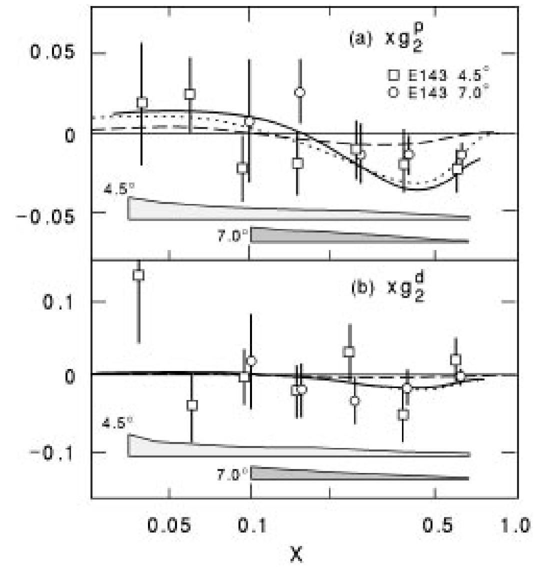

FIG. 2. Measurements for (a) xg_2^p and (b) xg_2^d from E143. Systematic errors are indicated by bands. Overlapping data have been shifted slightly in x to make errors clearly visible. The solid curve shows the twist-2 g_2^{WW} calculations for $E = 29.1$ GeV and $\theta = 4.5°$. The same curve for 7° is nearly indistinguishable. Bag model calculations at $Q^2 = 5.0$ (GeV$/c)^2$ by Stratmann [25] (dotted), and Song and McCarthy [16] (dashed) are indicated.

By extracting the quantity $\overline{g_2}(x, Q^2) = g_2(x, Q^2) - g_2^{WW}(x, Q^2)$, we can look for possible quark mass and higher twist effects. If the term in Eq. (1) which depends on quark masses can be neglected then $\overline{g_2}(x, Q^2)$ is entirely twist-3. Our results can be seen from the difference between the data and the solid line in Fig. 2. Within the experimental uncertainty the data are consistent with $\overline{g_2}$ being zero but also with $\overline{g_2}$ being of the same order of magnitude as g_2^{WW}.

Using our results for the longitudinal spin structure functions g_1^p and g_1^d, we have computed the first few moments of the OPE sum rules, and solved for the twist-3 matrix elements d_n. These moments are defined to be $\Gamma_1^{(n)} = \int_0^1 x^n g_1(x)dx$ and $\Gamma_2^{(n)} = \int_0^1 x^n g_2(x)dx$. For the measured x region, we evaluated g_1 and corrected the twist-2 part of g_2 to fixed $Q^2 = 5$ (GeV$/c)^2$, assuming g_1/F_1 is independent of Q^2 [24], and have averaged the two spectrometer results to evaluate the moments. Any possible Q^2 dependence of $\overline{g_2}$ has been neglected. We neglect the contribution from the region $0 \le x \le 0.029$ because of the x^n suppression factor. For $0.8 \le x \le 1$, we assume

TABLE I. Results for the moments $\Gamma_1^{(n)}$ and $\Gamma_2^{(n)}$ evaluated at $Q^2 = 5$ (GeV/c)^2, and the extracted twist-3 matrix elements d_n for proton (p) and deuteron (d) targets. The errors include statistical (which dominate) and systematic contributions.

	n	$\Gamma_1^{(n)} \times 10^3$	$\Gamma_2^{(n)} \times 10^3$	$d_n \times 10^3$
p	2	12.1 ± 1.0	−6.3 ± 1.8	5.4 ± 5.0
	4	3.2 ± 0.4	−2.3 ± 0.6	0.7 ± 1.7
	6	1.2 ± 0.2	−1.0 ± 0.3	0.1 ± 0.8
d	2	4.0 ± 0.8	−1.4 ± 3.0	3.9 ± 9.2
	4	0.8 ± 0.3	0.0 ± 1.0	1.7 ± 2.6
	6	0.2 ± 0.2	0.1 ± 0.5	0.6 ± 1.1

that both g_1 and g_2 behave as $(1-x)^3$ [26], and we fit data with $x > 0.56$. The uncertainty in the extrapolated contribution is taken to be the same as the contribution itself. The results are shown in Table I. We find that using the alternate assumption that A_1 and A_2 are independent of Q^2 introduces a sensitivity in Q^2 to the d_n results which is not present when assuming g_1/F_1 is independent of Q^2. In Table II we quote theoretical predictions [16,25,27,28] for d_2^p and d_2^d. For d_2^d the proton and neutron results were averaged, and a deuteron D-state correction was applied. Our results for d_n are consistent with zero, but the errors are large. The precision of the data is insufficient to distinguish between model predictions. We have also evaluated the integrals $\int_{0.03}^1 g_2^p(x)dx = -0.013 \pm 0.028$ and $\int_{0.03}^1 g_2^d(x)dx = -0.033 \pm 0.082$ using the same high-x extrapolation as discussed above. These results are consistent with zero.

In summary, we have measured the proton and deuteron spin structure function g_2 and virtual photon-nucleon asymmetry A_2 as a function of x at two different Q^2. We find that A_2 is significantly smaller than the $\sqrt{R}$ limit. We also find that $A_2 > 0$ for the proton. Within errors, g_2 is consistent with the twist-2 g_2^{WW} calculation as well as with some theoretical predictions [16,25]. The component $\overline{g_2}$ is consistent with zero, but also with $\overline{g_2}$ being of the same order of magnitude as g_2^{WW}. Twist-3 matrix elements d_2 have been evaluated, and are consistent with zero within errors. More precise data on g_2 are needed in order to make any conclusions regarding possible twist-3 and quark-mass-dependent contributions.

We wish to thank N. Shumeiko for help with the radiative corrections, and R. Jaffe and J. Ralston for useful discussions. This work was supported by DOE Contracts No. DE-AC05-84ER40150, No. W-2705-Eng-48, No. DE-FG05-94ER40859, No. DE-AC03-76SF00515, No. DE-FG03-88ER40439, No. DE-FG05-88ER40390, No. DE-FG05-86ER40261, and No. DE-AC02-76ER00881; NSF Grants No. 9114958, No. 9307710, No. 9217979, No. 9104975, and No. 9118137; the Commonwealth of Virginia; the Centre National de la Recherche Scientifique and the Commissariat a l'Energie Atomique (French groups); and the Japanese Ministry of Education, Science, and Culture.

TABLE II. Theoretical predictions for the twist-3 matrix element d_2^p for proton and d_2^d for deuteron.

	Bag models		QCD sum rules	
	Ref. [16]	Ref. [25]	Ref. [27]	Ref. [28]
Q^2 (GeV/c)^2	5	5	1	1
$d_2^p \times 10^3$	17.6	6.0	−6 ± 3	−3 ± 6
$d_2^d \times 10^3$	6.6	2.9	−17 ± 5	−14 ± 6

*Present address: California Institute of Technology, Pasadena, CA 91125.
†Permanent address: Oliver Lodge Lab, University of Liverpool, Liverpool, UK.
‡Permanent address: University of Bonn, D-53113 Bonn, Germany.
§Present address: College of William and Mary, Williamsburg, VA 23187.
‖Permanent address: FFIYM, P.O. Box 25, N-2007 Kjeller, Norway.
¶Present address: Kent State University, Kent, OH 44242.
**Permanent address: CERN, 1211 Geneva 23, Switzerland.

[1] EMC Collaboration, J. Ashman *et al.*, Phys. Lett. B **206**, 364 (1988); Nucl. Phys. **B328**, 1 (1989).
[2] SMC Collaboration, D. Adams *et al.*, Phys. Lett. B **329**, 399 (1994); **336**, 125 (1994); **357**, 248 (1995).
[3] E142 Collaboration, P. L. Anthony *et al.*, Phys. Rev. Lett. **71**, 959 (1993).
[4] E143 Collaboration, K. Abe *et al.*, Phys. Rev. Lett. **74**, 346 (1995).
[5] E143 Collaboration, K. Abe *et al.*, Phys. Rev. Lett. **75**, 25 (1995).
[6] J. Ellis and R. Jaffe, Phys. Rev. D **9**, 1444 (1974); **10**, 1669 (1974).
[7] J. D. Bjorken, Phys. Rev. **148**, 1467 (1966); Phys. Rev. D **1**, 1376 (1970).
[8] J. Ellis and M. Karliner, Phys. Lett. B **341**, 397 (1995).
[9] R. L. Jaffe and X. Ji, Phys. Rev. D **43**, 724 (1991).
[10] E. V. Shuryak and A. I. Vainshtein, Nucl. Phys. **B201**, 141 (1982).
[11] L. Mankiewicz and Z. Rysak, Phys. Rev. D **43**, 733 (1991).
[12] X. Artru and M. Mekfi, Z. Phys. C **45**, 669 (1990).
[13] J. L. Cortes, B. Pire, and J. P. Ralston, Z. Phys. C **55**, 409 (1992).
[14] S. Wandzura and F. Wilczek, Phys. Lett. **72B**, 195 (1977).
[15] R. L. Jaffe and X. Ji, Phys. Rev. Lett. **67**, 552 (1991).
[16] X. Song and J. S. McCarthy, Phys. Rev. D **49**, 3169 (1994); **50**, 4718 (1994); X. Song, Report No. INPP-UVA-95/04 (unpublished).
[17] H. Burkhardt and W. N. Cottingham, Ann. Phys. **56**, 453 (1970).
[18] M. Anselmino, A. Efremov, and E. Leader, Phys. Rep. **262**, 1 (1995).

[19] T. V. Kukhto and N. M. Shumeiko, Nucl. Phys. **B219**, 412 (1983); I. V. Akusevich and N. M. Shumeiko, J. Phys. G **20**, 513 (1994).
[20] Y. S. Tsai, Report No. SLAC-PUB-848 (unpublished); Rev. Mod. Phys. **46**, 815 (1974).
[21] NMC Collaboration, P. Amaudruz *et al.*, Phys. Lett. B **295**, 159 (1992).
[22] L. W. Whitlow *et al.*, Phys. Lett. B **250**, 193 (1990).
[23] B. Ehrnsperger and A. Schafer, Phys. Rev. D **52**, 2709 (1995).
[24] E143 Collaboration, K. Abe *et al.*, Phys. Lett. B **364**, 61 (1995).
[25] M. Stratmann, Z. Phys. C **60**, 763 (1993), and private communication for values at $Q^2 = 5$ (GeV$/c$)^2.
[26] A. Ali, V. M. Braun, and G. Hiller, Phys. Lett. B **266**, 117 (1991).
[27] E. Stein *et al.*, Phys. Lett. B **343**, 369 (1995).
[28] I. I. Balitsky, V. M. Braun, and A. V. Kolesnichenko, Phys. Lett. B **242**, 245 (1990); **318**, 648 (1993).